Optically detected magnetic resonance studied via the blue luminescence of Ti-doped Al_2O_3

1998 J. Phys.: Condens. Matter 10 4297

(http://iopscience.iop.org/0953-8984/10/19/017)

J. Phys.: Condens. Matter **10** (1998) 4297–4306. Printed in the UK PII: S0953-8984(98)91318-2

Optically detected magnetic resonance studied via the blue luminescence of Ti-doped Al_2O_3

E Ruža†, H J Reyher‡§, J Trokšs† and M Wöhlecke‡

† University of Latvia, Institute of Solid State Physics, Kengaraga Street 8, LV-1063 Riga, Latvia

‡ FB Physik, Universität Osnabrück, D-49069 Osnabrück, Germany

Received 3 February 1998

Abstract. The UV-excited blue and green luminescence bands of Ti:sapphire are characterized by ODMR. These emission bands are attributed to two Ti^{3+}–O^- centres, which show very similar properties and are created as a result of a charge-transfer transition of an electron from O^{2-} to Ti^{4+} ions. In both centres, the d electron of Ti^{3+} and the hole of O^- are strongly coupled and form triplet states. Doublet systems can be ruled out as sources of the blue–green luminescence. The angular dependence of the ODMR can be explained with an appropriate spin Hamiltonian assuming orthorhombic local symmetry. The orientation of the principal axes of the *g*-tensor and the crystal-field tensor, found for both centres, suggest that the hole is localized on a single oxygen ion and that the Ti^{3+}–O^- bond is almost aligned with the Al–O bonds of the undisturbed lattice.

1. Introduction

Titanium-doped Al_2O_3 is an important solid-state laser material [1] with a wide tunable spectral range from 0.7 to 1.1 μm, which is related to the vibrationally broadened T $\longleftrightarrow$ E crystal-field transition of Ti^{3+} ions. The success of this laser triggered renewed interest in the absorption and emission properties of solids in general and in particular for systems similar to Ti:sapphire. Research focused mainly on parasitic absorption bands and on new emission bands, which are most interesting if shifted to shorter wavelengths with respect to those for Ti:sapphire. In this respect, $YAlO_3$, for example, has been investigated intensively as a promising host material [2]. Likewise, transitions of titanium-doped Al_2O_3 other than T $\longleftrightarrow$ E have been examined thoroughly, especially those related to the so-called blue luminescence of sapphire, which is the subject of the present paper.

The UV-excited blue emission of Ti:sapphire consists of a band 100 nm wide, peaking at 420 nm. It was described only in 1985 as a result of room temperature experiments for an as-grown crystal and was attributed to Ti^{4+}, because it could be reduced substantially in favour of the Ti^{3+} NIR emission band by thermal annealing [3]. Later [4], it was found that the blue emission band at 420 nm is accompanied by a 'green' emission band, peaking at $\approx$460 nm, which was attributed to the 3d $\longleftrightarrow$ 4s transition of Ti^{3+}. The new band is covered by the blue one at room temperature and becomes visible only at lower temperatures due to a shift of the relative intensities of both bands. Also the lifetimes of both emissions are different, that is, 47 μs for the 'green' and 1.4 ms for the 'blue' band at 10 K [4]. The

§ Author to whom any correspondence should be addressed; fax: +49-541-9692670; e-mail: hjreyher@physik.uni-osnabrueck.de.

0953-8984/98/194297+10$19.50

latter feature may be used to disentangle the two bands using time-resolved spectroscopy [4]. A similar finding was reported by Wong *et al* [5], the green band, however, showing a maximum at 520 nm under 240 nm excitation. In reference [4], the green band was attributed to a Ti^{4+} transition based on the comparison of three samples with different $[Ti^{3+}]/[Ti^{4+}]$ concentration ratios. Another earlier paper [6] gives the same attribution and reports on the separation of the green and blue emission (here peaking at 480 and 410 nm, respectively) by means of different spectral dependences of the excitation. On the basis of several indirect arguments, the latter two references assume a charge-transfer transition

$$Ti^{4+} + O^{2-} \longleftrightarrow Ti^{3+} + O^{-}$$

to be responsible for the green as well as for the blue emission band.

The results of the present paper will show that these assumptions are essentially correct. The recently given alternative explanation for the blue emission of Ti:sapphire invoking F^{+} centres [7] is not supported by our findings.

2. Experimental details

The specimen used in our experiments was taken from a collection in our department. The growth process and the nominal Ti content are not known. In EPR measurements at X-band frequencies we found only the signal of the isolated Ti^{3+} ion [6]. Also the room temperature absorption spectra showed no traces of impurities other than Ti. Besides the well-known Ti^{3+} band around 500 nm, only a shoulder in the UV is found, which is characteristic for Ti^{4+} [8]. From this we assume pure Ti doping. We may further estimate the Ti^{3+} and Ti^{4+} concentration according to reference [8] from the absorption coefficients at the peak of the T $\longleftrightarrow$ E transition (Ti^{3+}) and at 45 000 cm^{-1} (Ti^{4+}). In this way we attain for our sample $[Ti^{3+}] \approx 4 \times 10^{18}$ cm^{-3} and $[Ti^{4+}] \approx 0.7 \times 10^{18}$ cm^{-3}.

The rectangular sample had a size of $2 \times 2.5 \times 5$ mm^3. The polished surfaces were oriented with the help of Laue photographs; they were (0001), $(10\bar{1}0)$ and $(\bar{1}2\bar{1}0)$ planes.

There are two techniques mainly applied for ODMR via luminescence [9]. Either the light polarization or the total intensity is observed. The latter method is especially suitable for triplet–singlet recombination systems and has been applied in this work.

Our experiment is designed as a standard set-up for ODMR via luminescence [9], consisting of a 6 T magnet–cryostat, a Xe lamp with a 10 cm monochromator (dispersion 8 nm mm^{-1}) for excitation and a 23 cm monochromator (dispersion 3.6 nm mm^{-1}) with an S20-type photomultiplier for the emission detection. For most of the ODMR measurements the monochromator in the detection path has been replaced by suitable filters to improve the signal-to-noise ratio. The excitation and detection arms are, as usual, at right angles, the optical path for detection being parallel to the magnetic field. The output of a 100 mW Gunn diode operating at 34 GHz is fed into the cryostat by a waveguide. The sample is mounted on a turnable rod (for angle variation) inside the waveguide at a distance of a quarter wavelength from the short-circuited end. A cavity could not be used because of the limited space in our cryostat. The resulting loss in strength of the B_1-field had no serious impact on the ODMR signals for the system investigated. This was checked by test runs using a 1 W IMPATT diode. Placing the sample into the waveguide instead of using a cavity allows us to apply the modulation of the Gunn-diode frequency for lock-in detection. This technique yielded a better signal-to-noise ratio than the usually applied amplitude modulation. We calibrated the magnet by measuring the ODMR of Al_2O_3:Cr^{3+}, detected via the selective re-absorption mechanism [10].

3. Results

Since the ODMR measurements were performed at approximately 2 K, we present in figure 1 the UV-excited emission spectrum measured at this temperature.

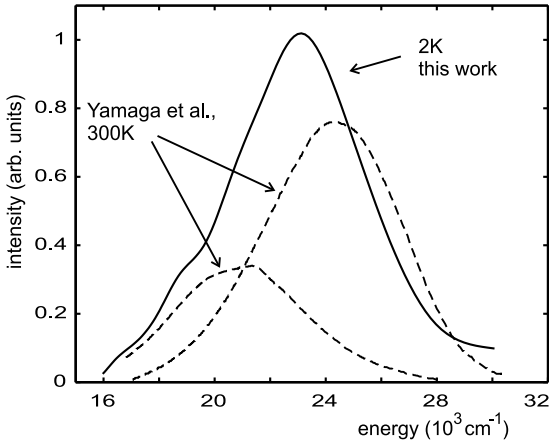

Figure 1. The emission spectrum of Al_2O_3:Ti under excitation with light at 40 800 cm^{-1}. The ordinate represents the photomultiplier current. For comparison the resolved blue and green luminescence bands from reference [6] are shown with arbitrary heights.

In agreement with the low-temperature data of reference [4], we observe a mixture of the green and the blue emission band. This is illustrated in a suggestive way by plotting in figure 1 the resolved bands from reference [6] with appropriate relative heights. The experimental values represent the photomultiplier current and have not been corrected for the sensitivity of the apparatus nor for the $(h\nu)^4$-dependence on the photon energy [11]. Hence, the curve does not represent a true line-shape, but rather allows comparison with the literature, where the above-mentioned corrections have not been applied, too.

For the emission spectrum shown in figure 1, the band of the exciting light was centred at 40 800 cm^{-1} and had a width of 5000 cm^{-1}. Because of this large bandwidth it was not possible to measure reliable excitation spectra. Using a filter covering the whole emission band, it was only possible to identify two maxima of the excitation efficiency, the more intense one being located at 40 800 cm^{-1} and the weaker one at 37 000 cm^{-1}. Taking into account our limited spectral resolution, this result is compatible with the emission spectra of reference [6], where two excitation bands centred at 39 200 and 36 700 cm^{-1} could be resolved at 300 K. A maximum at 37 700 cm^{-1} is reported in reference [12]. The deviation of our positions from these data may also result from the different temperatures applied. In view of this, we conclude from the comparison of our optical data with the literature† that we *do* observe the blue–green luminescence of Ti:sapphire and may now present the results of ODMR for this emission.

If ODMR is to be detected via a change of the overall intensity without polarization analysis, either an increase or a decrease of this intensity should be observed with rising magnetic field. Such changes arise from different probabilities for transitions from the individual Zeeman components of the starting level and from unequal population of these

† The excitation spectrum of reference [8], which shows a single maximum at 44 000 cm^{-1}, disagrees with our data and with the cited references as well. The reason for this discrepancy is unclear.

components, which may result from thermalization during the radiative lifetime. At 1.5 K we found an intensity decrease of several per cent at a field of 1 T.

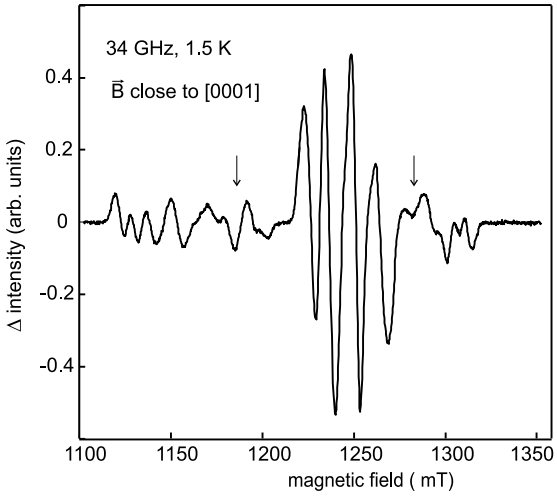

Figure 2. An ODMR spectrum of Al_2O_3:Ti for $\boldsymbol{B}$ close to [0001]. Excitation: 40 800 cm^{-1}; observation: 16 000–32 000 cm^{-1}. The ordinate represents the change of the photomultiplier current due to microwave transitions in the excited state. These changes have derivative-like shape because of the lock-in technique applied. Two signals corresponding to an increase of the luminescence intensity are marked by arrows.

Figure 2 shows the ODMR signals as a change of the detected intensity in the spectral range between 16 000 and 32 000 cm^{-1}, which corresponds to the full scale displayed in figure 1. Our analysis of the angular dependence of these signals, to be presented below, will show that all resonances can be explained by assuming two structurally different excited triplet centres T1 and T2. Both T1 and T2 have local orthorhombic symmetry and, hence, according to crystal symmetry, occur in six orientations, which are magnetically inequivalent for a general direction of the magnetic field. This explains the large number of resonance lines to be seen in figure 2. Except for the $\Delta M_S = 2$ transitions at half-field, typical for triplet systems, no further ODMR lines were observed.

One may note that two signal phases can be seen in figure 2, one yielding the dominating 'up–down' structure and the other giving 'down–up' signals, the latter being marked by arrows. This feature arises from the fact that ODMR signals corresponding to a decrease (absorptive) and an increase (emissive) of the luminescence intensity are present. By direct observation without a lock-in amplifier, we checked that the majority of the observed resonances are emissive. In principle, information of this kind may be useful in setting up a detailed model describing the spin–orbit states and the recombination mechanism, as has been done, e.g., in the well-known ODMR work on F centres in CaO [13]. However, such an analysis requires additional information on the polarization of the emission. This task has not been tackled because of the much more complicated symmetry conditions here compared to those for F centres in CaO. We shall not comment further on the ODMR signs in this report.

Using the same experimental conditions as for the ODMR spectrum in figure 2, we measured the angular dependence for rotations of the magnetic field in two perpendicular planes, namely the (0001) and the $(10\bar{1}0)$ plane. The positions of the resonances found experimentally are shown in figure 3 as open circles (emissive signals) and crosses

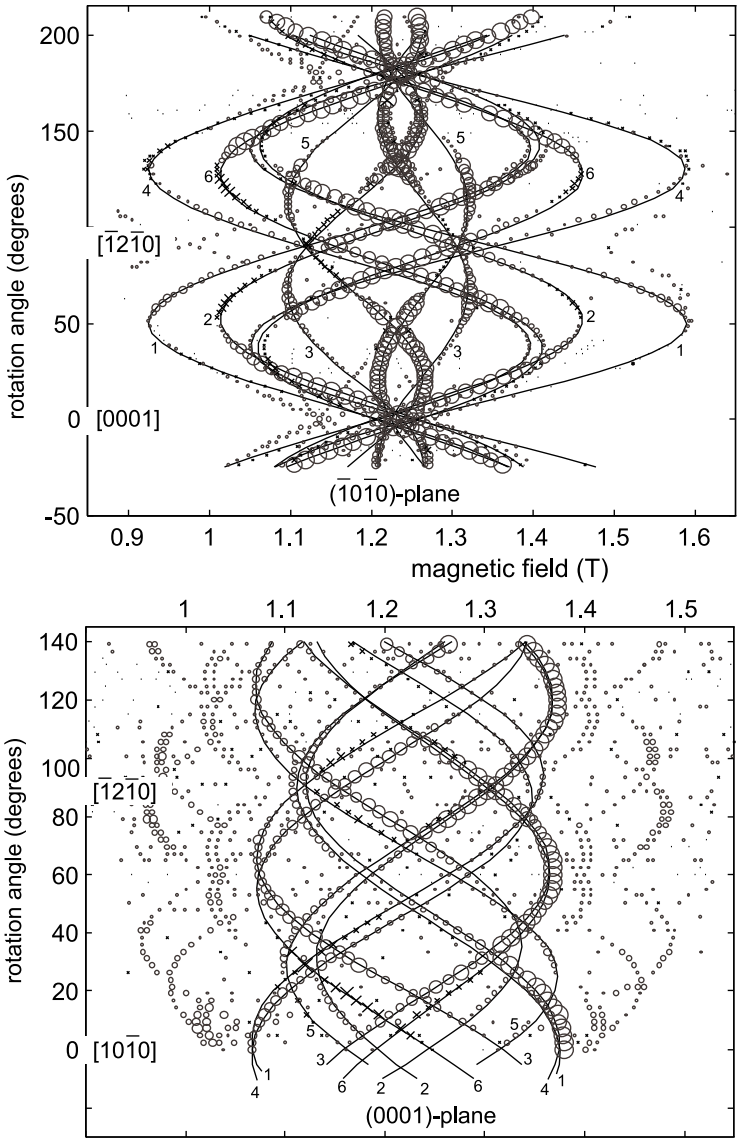

Figure 3. The angular dependence of the ODMR signals at 34 GHz (circles: emissive; crosses: absorptive) for rotations of $\boldsymbol{B}$ in the (10$\bar{1}$0) and the (0001) plane. The lines indicate calculated resonance positions according to a fit for triplet system T1. Experimental points not subjected to line fitting belong to triplet system T2, the fit not being shown, for clarity. The numbers refer to the orientations of the centres as given in table 1. The resonances of T2 could be better resolved for a rotation in (0001), because the luminescence intensity was higher for this orientation of the crystal.

(absorptive signals).

Solid lines represent a fit for centre T1 using the spin Hamiltonian to be described in the next paragraph. The fit for centre T2 is not shown for the sake of clarity. Therefore the corresponding points are not accompanied by lines representing the fit.

The patterns displayed in figure 3 are typical for systems with $S = 1$, as is the existence of resonance lines at half-field corresponding to $\Delta M_S = 2$ transitions mentioned above. Satisfactory fits to the data points could be achieved by assuming triplet centres with at least orthorhombic local symmetry. For this situation the appropriate spin Hamiltonian is given with respect to the principal axes of the centre under consideration by

$$H = \mu_{\mathrm{Bohr}} B(l g_x S_x + m g_y S_y + n g_z S_z) + D(3S_z^2 - S(S+1)) + E(S_x^2 - S_y^2).$$

Here, l, m, n are the projection cosines of the magnetic field $\boldsymbol{B}$ onto the centre's principal axes $\hat{\boldsymbol{x}}, \hat{\boldsymbol{y}}, \hat{\boldsymbol{z}}$, and D and E are the usual symmetry-allowed crystal-field parameters [14]. The results for D, E, and $g_{x,y,z}$ are listed in table 1. There, we also indicate the Eulerian angles α, β, γ, which describe the orientations of the principal-axes systems S of the triplet centres with respect to a rectangular crystal coordinate system S_0 being given by $\hat{\boldsymbol{x}}_0 \parallel [10\bar{1}0]$, $\hat{\boldsymbol{y}}_0 \parallel [\bar{1}2\bar{1}0]$, and $\hat{\boldsymbol{z}}_0 \parallel [0001]$. These angles are defined in the usual way, α describing a rotation around $\hat{\boldsymbol{z}}_0$ yielding the first intermediate system S_1, β around $\hat{\boldsymbol{y}}_1$ giving S_2, and γ the final rotation around $\hat{\boldsymbol{z}}_2$ leading to S. Later we shall relate these directions of the centre axes to the crystal structure. In fact, only three angles were used as fitting variables, which describe the orientation of one orthorhombic triplet centre. The orientations and, hence, the angles of the other five structurally equivalent centres are then determined by the host crystal symmetry. In particular this means: $\alpha_2 = \alpha_1 + 120^\circ$, $\alpha_3 = \alpha_1 + 240^\circ$, $\alpha_4 = 90^\circ - \delta$, $\alpha_5 = \alpha_4 + 120^\circ$, $\alpha_6 = \alpha_4 + 240^\circ$; $\beta_{2,3} = \beta_1$, $\beta_4 = \beta_{5,6} = 180^\circ - \beta_1$; $\gamma_{2,\ldots,6} = \gamma_1$. Of course, other angles could be chosen corresponding to interchanged axes $\hat{\boldsymbol{x}}, \hat{\boldsymbol{y}}, \hat{\boldsymbol{z}}$. The listed values were preferred, since D is larger than E in the thus-defined coordinate system. This emphasizes the predominant axial character of the local crystal field. Both values for D and E were arbitrarily taken to be positive. The sign of D cannot be found from angular dependencies, but requires the study of the ODMR signs mentioned above. Finally, the sign of E may always be changed by interchanging the local x- and y-axes.

Table 1. Values of the spin-Hamiltonian parameters. x, y, z refer to the principal-axes system of the triplet centres. Equivalencies [15]: $b_{20} = D$, $b_{22} = 3E$. The orientation of the centre No 1 (referring to the branches in figure 3) is indicated by Euler angles; the directions for the other five structurally equivalent centres result from crystal symmetry (see the text). The errors have been estimated by single-parameter variation which leads to a 15% increase of the residual deviation persisting in the best-fit case. This corresponds to a clearly visible deterioration of the fit.

Triplet centre	$g_{x,y,z}$	D, E (10^{-4} cm^{-1})	α, β, γ
T1	1.999(5), 1.958(5), 1.941(5)	3060(30), 340(20)	$90^\circ + \delta$ with $\delta = 9.3(4)^\circ$, $50.4(3)^\circ$, $-55(2)^\circ$
T2	1.985(5), 1.987(5), 1.985(5)	3420(60), 540(40)	$90^\circ + \delta$ with $\delta = -2.7(6)^\circ$, $62.7(6)^\circ$, $-44(3)^\circ$

The data in table 1 will be discussed in the next section. Before doing so, we want to add some comments on the fitting process. All branches of the angular dependencies for both planes have been fitted simultaneously using a MATLAB program. This procedure yielded significant values for the fitting parameters, since the experimental information is clearly sufficient in view of the number of parameters. The high sensitivity of the fit follows from the fact that substantial deviations from the experimental points persisted, unless the technically unavoidable small misalignment (of the order of 1°) of the crystal rotation axis was taken into account as a correction. In the lower part of figure 3 one may also recognize

that some branches of the T2 centres show a splitting near the extrema. This splitting has been ignored in the fit for T2, since its origin is currently not understood. It may result from the fact that there exist two very similar T2 centres, but it may also be an artifact due to a peculiar ODMR line-shape.

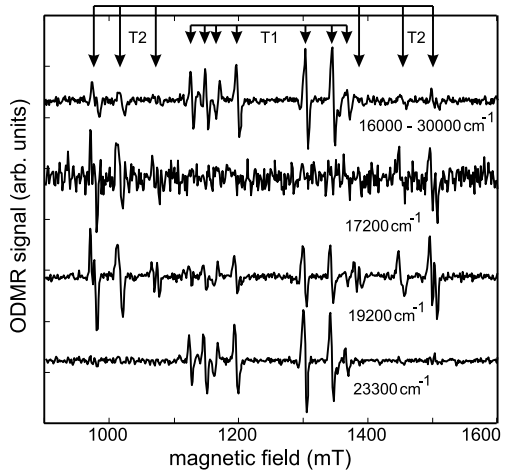

Figure 4. ODMR spectra for $\boldsymbol{B}$ approximately parallel to $[\bar{1}2\bar{1}0]$. The various energies of observations are indicated.

The ODMR spectra shown in figure 4 were detected using various filters, three interference filters (width $\approx$400 cm^{-1}) and a broad-band colour glass filter covering the whole region of emission. The crystal has been oriented such that $\boldsymbol{B}$ is near $[\bar{1}2\bar{1}0]$. For this orientation, the ODMR lines of both systems, T1 and T2, as indicated by arrows, are separated. It is evident that the lines of T2 are practically absent when observing at 23 300 cm^{-1}, while the lines of T1 are lost in noise for an observation energy of 17 200 cm^{-1}. For broad-band detection as well as for 19 200 cm^{-1} both centres show up, but T2 gains in intensity for the latter energy. Unfortunately we could not work with higher spectral resolution using a monochromator because of the then weak signal intensity. Nevertheless, with reference to figures 1 and 4 it is straightforward to attribute the green and blue luminescence bands to the triplet centres T2 and T1, respectively. This and the possible nature of these centres will be commented on in the next section.

Before doing so, we want to mention that, within error limits, we could not find for T1 and T2 a different dependence of the ODMR intensity on the microwave power. This is surprising since it is known that the blue and the green luminescence bands arise from states having very different radiative lifetimes τ [4]. The only explanation for this finding is to assume a spin–lattice relaxation time T_1 of the same order for both centres, which is short compared to τ for T2, the short-lived centre. In this case the ODMR intensity is not limited by τ but rather by T_1, thus explaining the above-mentioned fact that the behaviours of the two sets of ODMR signals are the same.

4. Discussion

As shown above, the observed ODMR spectra can well be understood by assuming two low-symmetry centres with excited triplet states. Furthermore there is evidence that these two centres, T1 and T2, are responsible for the blue and green luminescence, respectively,

of Al_2O_3:Ti. Because of the triplet character of the ODMR signals, doublet systems such as F^+ colour centres [7] or Ti^{3+} ions [4] can be ruled out as luminescence centres.

Since the ODMR data for T1 and T2 are very similar, it is plausible to assume one basic centre occurring in two modifications. This is exactly the situation described in references [6, 5]. Both papers postulate a Ti^{3+}–O^- pair as the emissive centre, which is created by an oxygen-to-Ti^{4+} charge-transfer transition. This multi-electron system may form an excited triplet state, most easily described as an electron–hole pair located at the respective ions. If the hole is indeed localized at a single oxygen ion, the resulting system including the nearest neighbours has C_1 symmetry. Then, if such a centre is approximated by an orthorhombic one, as we have done in our ODMR analysis, one principal axis should be directed almost parallel to the Ti–O bond. This is the case for the local z-axes of both T1 and T2, as we shall explain now.

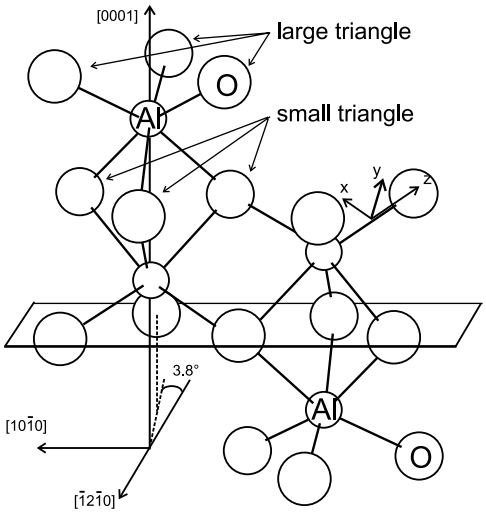

Figure 5. The fraction of the Al_2O_3 lattice showing the four inequivalent Al sites. Ti is assumed to substitute for Al. The crystal axes are given at the bottom on the left. Aluminium ions are aligned on the [0001] axis; oxygen ions are grouped in small and large triangles in horizontal planes with respect to [0001]. The approximate orientation of a local coordinate system found for T1 and T2 is shown at an arbitrarily selected Al–O bond.

From table 1 we read off 99.3°/87.3° and 50.4°/62.7° for α and β, which describe the direction of $\hat{\boldsymbol{z}}$ with respect to $[10\bar{1}0], [\bar{1}2\bar{1}0], [0001]$. These values have to be compared with α =93.8°/90° and β = 64.4°/47° for the direction $\hat{\boldsymbol{b}}$ of the Al–O bonds of the large and the small 'oxygen triangles', respectively, as calculated from structure data [16]. The situation is depicted in figure 5, where the coordinate system of a T1 (or T2) centre is shown schematically. It is surely not accidental that the principal axes $\hat{\boldsymbol{z}}$ of the T1 and T2 centres and the Al–O bond directions $\hat{\boldsymbol{b}}$ are nearly aligned. Rather, this finding gives strong evidence supporting the Ti^{3+}–O^- model for the blue–green luminescence of Ti:sapphire [6, 5].

The direction of $\hat{\boldsymbol{x}}$ and $\hat{\boldsymbol{y}}$ cannot be related in an equally simple manner to the local geometry. This is anyway not to be expected since the orthorhombic character of the fragment consisting of Ti–O and the seven nearest-neighbour ions is determined by a rather complicated arrangement of these ions. We may note, however, that this fact does not influence the argumentation just given concerning the $\hat{\boldsymbol{z}}$-axis.

Without further information it seems too speculative to attribute the oxygen ion of the Ti^{3+}–O^- centres to either the large or the small oxygen triangle. One has to expect relaxation of the centre after the charge transfer, and this fact complicates such an attribution. Also a local distortion by a defect associated with Ti cannot be ruled out, at present. This situation has been invoked for the green luminescence centre by references [6, 5] to explain its shorter lifetime.

Unfortunately we cannot present a model calculation describing the values of the observed g-tensors. Instead we will argue qualitatively and outline the complications to be expected in a corresponding calculation. As mentioned above, one may conceive the excited multi-electron state of Ti^{3+}–O^- as a hole and a single electron, which are strongly coupled and form a triplet state. Hence, the g-values are determined by a 'mixture' of contributions from Ti^{3+} and O^- states. Holes on oxygen ions in an axial (or orthorhombic) environment in oxides typically have slightly anisotropic g-values, somewhat larger than the free-electron value [17]. Isolated Ti^{3+} in Al_2O_3 has $g_\perp < 0.1$ and $g_\parallel = 1.067$ [18], where the directions refer to the [0001] axis of the crystal. These highly asymmetric g-values arise from the presence of orbital momentum in the ground state of this d^1 ion [14]. In the axial crystal field of C_3 symmetry the orbital doublet E is the lowest state. If a symmetry-lowering neighbour defect, like O^-, is present, one has to expect quenching of the orbital momentum. The orbital states of the d^1 ion then correspond to non-degenerate single-valued irreducible representations of the appropriate low-symmetry group. The g-values will then become similar to those of Ti^{3+} in the isostructural $LiNbO_3$, where the trigonal crystal field is such that an orbital singlet (A_1 state) is lowest. Here, one finds $g_\perp = 1.84$ and $g_\parallel = 1.96$ [19]. An even more comparable case was described in reference [6]: in redox-treated Al_2O_3 samples, a Ti^{3+} centre of low symmetry with a g-tensor very similar to that of our triplet centres was found ($g_{x,y,z} = 1.82, 1.88, 1.94$ with $\alpha = 0^\circ$, $\beta = 56^\circ$, $\gamma = 0^\circ$ for the local centre axes). In view of these facts, the observed values for the g-tensors of the T1 and T2 triplet centres are not surprising at all. An actual calculation will be rather elaborate because one has not only to set up the lowest excited state, from which the emission starts, but also the states somewhat higher in energy. These states are admixed by the Zeeman effect and may affect the g-values strongly. The situation will be further complicated by orbital reduction effects due to covalency.

5. Summary and conclusion

In summary we have confirmed the Ti^{4+} model for the blue–green luminescence of references [6, 5]. Our ODMR results give direct evidence that this luminescence stems from Ti^{4+} ions, which are most probably located on Al sites. The excited configuration results from a UV-induced transfer of an electron from oxygen to Ti^{4+} and may be described as a strongly coupled electron–hole system Ti^{3+}–O^-. The lowest excited state of this configuration is a triplet system exhibiting at least orthorhombic local symmetry. The latter fact and the orientation of the principal axes of the spin-Hamiltonian tensors suggest that the hole is localized on a neighbouring oxygen ion and that the Ti^{3+}–O^- bond is oriented mainly parallel to the Al–O bonds of the perfect lattice. The triplet centre described occurs in two modifications T1 and T2, which are connected with the blue and the green luminescence bands, respectively.

It is true that we investigated only one sample, but the results are unambiguous. There is no reason to assume that significantly different findings are to be expected for other specimens. Therefore we think the issue concerning the blue luminescence of Al_2O_3:Ti to be settled.

It has been claimed in reference [7] that the simultaneous presence of both charge states Ti^{3+} and Ti^{4+} prevents us from using Ti:sapphire as a laser material in the blue spectral region. Self-absorption from the unavoidable Ti^{3+} ions would hinder possible laser action. Since we have shown that the blue luminescence is due to Ti ions and does not result from F^+ centres created by Ti doping, it is not possible to replace Ti by another doping material, as is proposed in reference [7]. Rather one has to lower the Fermi level by co-doping with suitable acceptors, whereupon Ti^{3+} is driven into the 4+ charge state.

In conclusion we want to note that we have given an example which shows that the ODMR method is well suited to the investigation of the luminescence properties of laser-active materials. In this particular field it has not yet been applied very often.

Acknowledgments

We thank Professor O F Schirmer for his steering interest and continuous support. JT thanks the DAAD for a grant. The financial support of the Deutsche Forschungsgemeinschaft (Graduiertenkolleg 'Mikrostruktur oxidischer Kristalle') is gratefully acknowledged.

References

[1] Gan Fuxi 1995 *Laser Materials* (Singapore: World Scientific)
[2] Basun S A, Danger T, Kaplyanskii A A, McClure D S, Petermann K and Wong W C 1996 *Phys. Rev.* B **54** 6141 and references therein
[3] Powell R C, Caslavsky J L, AlShaieb Z and Bowen J M 1985 *J. Appl. Phys.* **58** 2331
[4] Macalik B, Bausá L E, García-Solé J, Jaque F, Muñoz Santiuste J E and Vergara I 1992 *Appl. Phys.* A **55** 144
[5] Wong W C, McClure D S, Basun S A and Kokta M R 1995 *Phys. Rev.* B **51** 5693
[6] Yamaga M, Yosida T, Hara S, Kodama N and Henderson B 1994 *J. Appl. Phys.* **75** 1111
[7] Chen W, Tang H, Shi Ch, Deng J, Shi J, Zhou Y, Xia Sh, Wang Y and Yin Sh 1995 *Appl. Phys. Lett.* **67** 317
[8] Wong W C, McClure D S, Basun S A and Kokta M R 1995 *Phys. Rev.* B **51** 5682
[9] Spaeth J-M and Lohse F 1990 *J. Phys. Chem. Solids* **51** 861
[10] Geschwind S, Collins R J and Schawlow A L 1959 *Phys. Rev. Lett.* **3** 545
[11] Wojtowicz A J, Kazmierczak M, Lempicki A and Bartram R H 1989 *J. Opt. Soc. Am.* B **6** 1106
[12] Reisfeld R, Eyal M and Jørgensen K 1987 *Chimia* **41** 117
[13] Edel P, Hennies C, Merle D'Aubigné Y, Romestain R and Twarowski Y 1972 *Phys. Rev. Lett.* **28** 1268
[14] Abragam A and Bleaney B 1970 *Electron Paramagnetic Resonance of Transition Ions* (Oxford: Clarendon)
[15] Al'tshuler S A and Kozyrev B M 1974 *Electron Paramagnetic Resonance in Compounds of Transition Elements* (New York: Halsted)
[16] Newnham R E and de Haan Y M 1962 *Z. Kristall.* **117** 235
[17] Weil J A, Bolton J R and Wertz J E 1994 *Electron Paramagnetic Resonance* (New York: Wiley)
[18] Kask N E, Kornienko L S, Mandel'shtam T S and Prokhorov A M 1964 *Sov. Phys.–Solid State* **5** 1677
[19] Juppe S and Schirmer O F 1986 *Phys. Lett.* **117A** 150